Cellulose depolymerization using zinc chloride hydrate and solid acid catalysts

Cellulose

Paiva, Mateus F.; Albuquerque, Elise M.; de Souza, Priscilla M.; Bitter, Johannes H.; Vanhove, Guillaume et al

https://doi.org/10.1007/s10570-024-06107-0

This publication is made publicly available in the institutional repository of Wageningen University and Research, under the terms of article 25fa of the Dutch Copyright Act, also known as the Amendment Taverne.

Article 25fa states that the author of a short scientific work funded either wholly or partially by Dutch public funds is entitled to make that work publicly available for no consideration following a reasonable period of time after the work was first published, provided that clear reference is made to the source of the first publication of the work.

This publication is distributed using the principles as determined in the Association of Universities in the Netherlands (VSNU) 'Article 25fa implementation' project. According to these principles research outputs of researchers employed by Dutch Universities that comply with the legal requirements of Article 25fa of the Dutch Copyright Act are distributed online and free of cost or other barriers in institutional repositories. Research outputs are distributed six months after their first online publication in the original published version and with proper attribution to the source of the original publication.

You are permitted to download and use the publication for personal purposes. All rights remain with the author(s) and / or copyright owner(s) of this work. Any use of the publication or parts of it other than authorised under article 25fa of the Dutch Copyright act is prohibited. Wageningen University & Research and the author(s) of this publication shall not be held responsible or liable for any damages resulting from your (re)use of this publication.

For questions regarding the public availability of this publication please contact openaccess.library@wur.nl

Cellulose
https://doi.org/10.1007/s10570-024-06107-0

ORIGINAL RESEARCH

Cellulose depolymerization using zinc chloride hydrate and solid acid catalysts

Mateus F. Paiva · Elise M. Albuquerque · Priscilla M. de Souza · Johannes H. Bitter · Guillaume Vanhove · Robert Wojcieszak · Fábio B. Noronha

Received: 28 April 2024 / Accepted: 2 August 2024

Abstract Increasing the efficiency of cellulose hydrolysis is a crucial milestone to enable its use as a platform for the production of renewable chemicals. Consequently, exploring alternative techniques for cellulose dissolution and subsequent depolymerization and hydrolysis remains a pivotal area of research. This study delves into the performance of diverse solid acid catalysts (ion-exchange resins, metal oxides, and zeolites) for cellulose depolymerization when combined with a concentrated solution of zinc chloride ($ZnCl_2$) as the reaction medium and extractant. The influence of this molten salt hydrate on cellulose dissolution and the stability of the tested catalysts was thoroughly investigated. Optimal mild operating conditions (90 °C and 2 h) that facilitate enhanced conversion and selective glucose production were identified. The highest glucose yields (exceeding 40%) were obtained with Amberlyst-15 and HZSM-5 ($SiO_2/Al_2O_3 = 23$), effectively mitigating product degradation and equaling or surpassing the traditional homogeneous system using H_2SO_4. Furthermore, insights into the deactivation mechanisms affecting the best catalysts are provided.

Keywords Cellulose hydrolysis · Molten salt hydrate · $ZnCl_2$ · Solid acid catalysts · Catalyst stability

Introduction

The hydrolysis of cellulose contained in lignocellulosic biomass produces glucose, a platform sugar that can be converted into high value-added chemicals and renewable fuels. The production of glucose from cellulose hydrolysis may be performed using enzymes,

---

Supplementary Information The online version contains supplementary material available at https://doi.org/10.1007/s10570-024-06107-0.

M. F. Paiva · E. M. Albuquerque · P. M. de Souza · R. Wojcieszak · F. B. Noronha (✉)
UMR 8181 – UCCS – Unité de Catalyse et Chimie du Solide, CNRS, Centrale Lille, Univ. Lille, Univ. Artois, 59000 Lille, France
e-mail: fabio.bellot@int.gov.br

E. M. Albuquerque · F. B. Noronha
Catalysis, Biocatalysis and Chemical Processes Division, National Institute of Technology, Rio de Janeiro, RJ 20081-312, Brazil

J. H. Bitter
Biobased Chemistry and Technology (BCT), Wageningen University & Research, P.O. Box 17, 6700 AA Wageningen, The Netherlands

G. Vanhove
UMR 8522 - PC2A - Physicochimie Des Processus de Combustion Et de L'Atmosphère, CNRS, Univ. Lille, 59000 Lille, France

R. Wojcieszak
L2CM UMR 7053, CNRS, Université de Lorraine, F-5400 Nancy, France

homogeneous acids, or solid acids (Zeng and Pan 2022). Currently, cellulases are expensive, difficult to recycle, and are not yet commercially viable. Inorganic acids (H_2SO_4 and HCl) are inexpensive, and they can perform cellulose hydrolysis efficiently. However, the hydrolysis catalyzed by concentrated or diluted acids still faces many issues such as: (i) challenging separation of acid and sugar and acid recovery; (ii) need for wastewater treatment; (iii) equipment corrosion; (iv) reduced sugar yield due to sugar degradation to 5-hydroxymethylfurfural (HMF), furfural, and levulinic acid (LA) under high operation temperature (Zhou et al. 2021; Zeng and Pan 2022). Solid acid catalysts emerged as a potential alternative to cellulose hydrolysis over traditional inorganic acids. They are less corrosive and more environmentally friendly than inorganic acids, and easier to recover and reuse, which makes them a sustainable choice. Despite these benefits, the challenge lies in their interaction with cellulose, due to the high cellulose crystallinity, the solid catalyst is blocked from reaching cellulose bonds, hindering efficient glucose production through hydrolysis. This bottleneck poses a significant obstacle for sugar platform based biorefineries. A promising pretreatment of cellulose involves the use of the so-called molten salt hydrates (MSH). This approach promotes cellulose dissolution and hydrolysis addressing the existing limitations (Rodriguez Quiroz et al. 2019a; Sun et al. 2022).

MSH are concentrated inorganic salt solutions with a water-to-salt molar ratio close to the coordination number of the strongest hydrated cation, with the water molecules bound to the inner coordination sphere of the cation, while the anion is free in solution (Leipner et al. 2000; Sen et al. 2016; Rodriguez Quiroz et al. 2019a). They are inexpensive, easier to prepare, and environmentally friendly since no toxic and volatile organic compounds are required to prepare such solvents. Moreover, the inorganic salts can be recovered by evaporating the water after cellulose regeneration and can be subsequently reused (Sen et al. 2013).

Inorganic molten salt hydrates are known to dissolve cellulose, which depends on the water content as well as the structure of the cation coordination sphere (Fischer et al. 2003; Sen et al. 2013). The cellulose solubility is attributed to the coordination of its primary OH group to the hydrated cation, replacing a water molecule in the inner coordination sphere of the metal-water coordination complex (Leipner et al. 2000; Sen et al. 2016; Rodriguez Quiroz et al. 2019b). The interaction between the cation and cellulose weakens and breaks the intra- and intermolecular hydrogen bonds of the cellulose chains. Different inorganic molten salt hydrates have been pointed out to dissolve cellulose such as: LiBr, LiCl, $ZnBr_2$, $ZnCl_2$, $FeBr_2$, and $FeCl_3$ (Leipner et al. 2000; Fischer et al. 2003; Chen et al. 2020).

The dissolution of cellulose in MSH decreases its crystallinity, which improves the reactivity of cellulose (Yang et al. 2014; Sun et al. 2022). Most of the studies about hydrolysis of cellulose with MSH in one or two steps use inorganic acids (Cao et al. 1994; Deng et al. 2015; Cheng et al. 2017; Rodriguez Quiroz et al. 2019b), organic acids (vom Stein et al. 2010) and heteropolyacids (Lara-Serrano et al. 2020) under mild conditions (low concentration of inorganic acid and temperature). Oligomers (Liu et al. 2021a, b; Ma et al. 2022a, b), glucose (de Almeida et al. 2010; Deng et al. 2015; Liang et al. 2022), fructose (Yoo et al. 2017), levoglucosan (Deng et al. 2015), HMF (Hou et al. 2017, 2021; Nie et al. 2020), and LA (Wei and Wu 2017; Lara-Serrano et al. 2020; Wang et al. 2020), are the main products formed, and the yield of each product depends on the type of MSH and reaction temperature (Sen et al. 2013; Deng et al. 2015; Yoo et al. 2017; Liu et al. 2019).

In spite of the large research efforts on the hydrolysis of cellulose using MSH in the presence of inorganic acids (e.g., H_2SO_4, HCl) (Paiva et al. 2024), only a few studies use solid acid catalysts (Wei and Wu 2017; Wu et al. 2020; Liang et al. 2022). Wei and Wu (2017) showed that it is possible to generate a synergic effect by applying $ZnCl_2$ and sulfated titania catalyst (SO_4/TiO_2), which contributes to cellulose depolymerization. They showed that the products can be adjusted by the control of reaction conditions. At low temperatures (80–100 °C), 90% of cellulose conversion was achieved, with a carbon balance of 83%, and a maximum glucose yield of 50.5%. At high temperatures (120–140 °C) and 2 h of reaction, LA was the major product (maximum yield 43.1%) and the carbon balance decreased to 73% due to the formation of insoluble humins. Unfortunately, the article does not discuss the stability/deactivation of the catalyst and recycling options (Wei and Wu 2017).

In another work, Wu et al. (2020) carried out the hydrolysis of cellulose at 140 °C for 8 h using a lithium bromide solution (60 wt.%) in the presence of BEA and ZSM-5 zeolites. Complete conversion of cellulose and a maximum glucose yield of 61% were obtained, having oligomers as by-products, with chains up to 10 glucose units, and HMF (yield of 4%). According to the authors, catalyst deactivation occurs via ion exchange between the H^+ of zeolite and the Li^+ cation in solution. A discussion about catalyst recycling was also addressed by the authors, who concluded that the zeolites could be recovered for a new reaction cycle with 50% of its initial activity after an ion exchange regeneration process (Wu et al. 2020).

More recently, Liang et al. (2022) reinforced the potential of using heterogeneous catalysts associated with MSH for cellulose hydrolysis. They used LiBr in the presence of corncob-derived carbon-base sulfonated catalysts. A high yield for glucose was achieved (80.1%) at 110 °C after a long reaction time (10 h), with the formation of LA (4%) as by-product. An evaluation of the reuse of the best catalyst was performed and indicated that most of the active sites were deactivated by leaching of $–SO_3H$ groups after the first reaction cycle (Liang et al. 2022). In those studies, only one catalyst with defined acidic properties was used.

The objective of this work is to carry out a systematic study of the effect of the nature and concentration of the acidic sites (Lewis and Brønsted) of heterogeneous catalysts on cellulose hydrolysis in the presence of MSH. In this way, acid solids containing only Lewis, Brønsted and both types of acid sites will be evaluated. Therefore, three different series of solid acid catalysts were studied: Ion-exchange polymer resins (Amberlys-15, Dowex 50 and Dowex 650), metal oxides ($NbOPO_4$, $Nb_2O_5 \cdot xH_2O$, m-ZrO_2, t-ZrO_2, WO_3/ZrO_2 and SO_3/ZrO_2) and zeolites (HZSM-5 containing different SiO_2/Al_2O_3 ratio (23, 55 and 280)). Furthermore, the potential mechanisms of catalyst deactivation are examined and discussed.

Experimental

Materials

Cellulose (Sigma-Aldrich, Sigmacell S5504), $ZnCl_2$ (Janssen Chimica), H_2SO_4 (Sigma-Aldrich), Amberlyst-15 (Sigma-Aldrich), Dowex 50 and Dowex 650 (Dow) were used in this work. Commercial oxides $Nb_2O_5 \cdot xH_2O$ and $NbOPO_4$ (CBMM), m-ZrO_2 ($<0.2\%$ SiO_2), t-ZrO_2 (3.3% SiO_2) and WO_3/ZrO_2 (Saint Gobain Norpro), SO_3/ZrO_2 (Mel Chemicals) and HZSM-5 zeolite (Zeolyst) containing different SiO_2/Al_2O_3 molar ratio (23, 55 and 280) were also investigated.

Catalysts characterization

X-ray diffraction (XRD) patterns of all catalysts were collected in a Brüker D8 Advance equipment using CuK_α radiation, with $\lambda = 1.54184$ Å. Diffractograms were obtained in the 2θ Bragg range between 5° and 80° with a scan rate of 0.02° $step^{-1}$ and scan time of 1 s $step^{-1}$.

Surface area and pore volume of the catalysts were evaluated by nitrogen adsorption and desorption isotherms in a Micromeritics ASAP 2020 at −196 °C. The specific surface area and total pore volume were calculated using the BET (Brunauer–Emmett–Teller) and BJH (Barrett, Joyner and Halenda) methods, respectively. Before the analysis, the samples were treated in situ under vacuum (9 mm Hg) at 350 °C for 8 h, to remove the adsorbed species.

The Brønsted acidity in the aqueous phase of the samples was estimated by titration following a method described by Kim et al. (2014), in which 0.05 g of catalyst were added to 20 mL of NaCl aqueous solution (1.0 mol L^{-1}) and dispersed for 1 h at room temperature with the aid of an ultrasonic bath. Then, the catalyst was removed by centrifugation and the resultant solution was filtrated and titrated with a NaOH aqueous solution (0.01 mol L^{-1}) using phenolphthalein as a neutralizing indicator.

In addition, the type of acid sites (Brønsted and Lewis) was assessed by Fourier Transform Infrared Spectroscopy using pyridine as probe molecule (Py-FTIR). The experiments were conducted using a Thermo Nicolet Protege 460 instrument with a CsI beam splitter and a MCT detector. Prior to the analysis, the sample self-supported wafer (2.0 cm^2) was treated at 450 °C under high vacuum overnight. Pyridine adsorption was performed at 100 °C until the equilibrium was reached and then, samples were evacuated at 150 °C under high vacuum for 30 min before the spectra acquisition. Brønsted and Lewis acid sites concentration was determined by the Lambert–Beer equation, using molar absorption coefficients of 1.67 cm μmol^{-1} and 2.22 cm μmol^{-1}, respectively.

Cellulose dissolution tests

Before the evaluation of the catalyst performance, tests involving only cellulose dissolution in the MSH were performed. Zinc chloride was selected for its wide availability and low cost when compared to the other inorganic molten salts. The solutions were prepared by mixing the appropriate amount of $ZnCl_2$ with deionized water to obtain $H_2O/ZnCl_2$ molar ratios (R) of 2.3, 3.0, 5.0, and 8.0 (76.7, 71.6, 60.2 and 48.6 wt.% of $ZnCl_2$ in the solution). Cellulose dissolution was then performed in a Radleys Carousel Reactor. For each experiment, 0.05 g of cellulose were added to 2.5 g of $ZnCl_2$ solution in a reaction flask with a stirring bar. The flask was sealed and placed in a Radleys Carousel station previously heated to 70 °C and kept at this temperature for the desired time under stirring (600 rpm).

Catalyst screening

Cellulose conversion experiments were carried out in the same Radleys Carousel Reactor. In a standard essay (Fig. 1), 0.05 g of substrate (cellulose) and 0.025 g or 0.05 g of catalyst were added to 2.5 g of $ZnCl_2$ solution containing H_2O/salt molar ratio of 3.0, in a reaction flask containing a stirring bar and placed in a Radleys Carousel station previously heated to the desired temperatures (70 or 90 °C) and kept at this condition throughout the whole reaction time (2–5 h) under stirring (600 rpm). After the reaction, the reaction flask was removed from the Radleys Carousel station and cooled down in a cold bath. Catalysts were then separated from the media by centrifugation and an aliquot of 0.3 g of the resulting hydrolysate was diluted 10 times for product analysis (Liu et al. 2019).

The reaction products from cellulose hydrolysis were analyzed by high-performance liquid chromatography (HPLC) using a Shimadzu Nexus equipped with a refractive index detector (RID) at 39 °C and a diode array detector (DAD) at 265 nm. A Phenomenex ROA-Organic Acids column was used at 30 °C in isocratic elution mode (0.6 mL min^{-1}) with

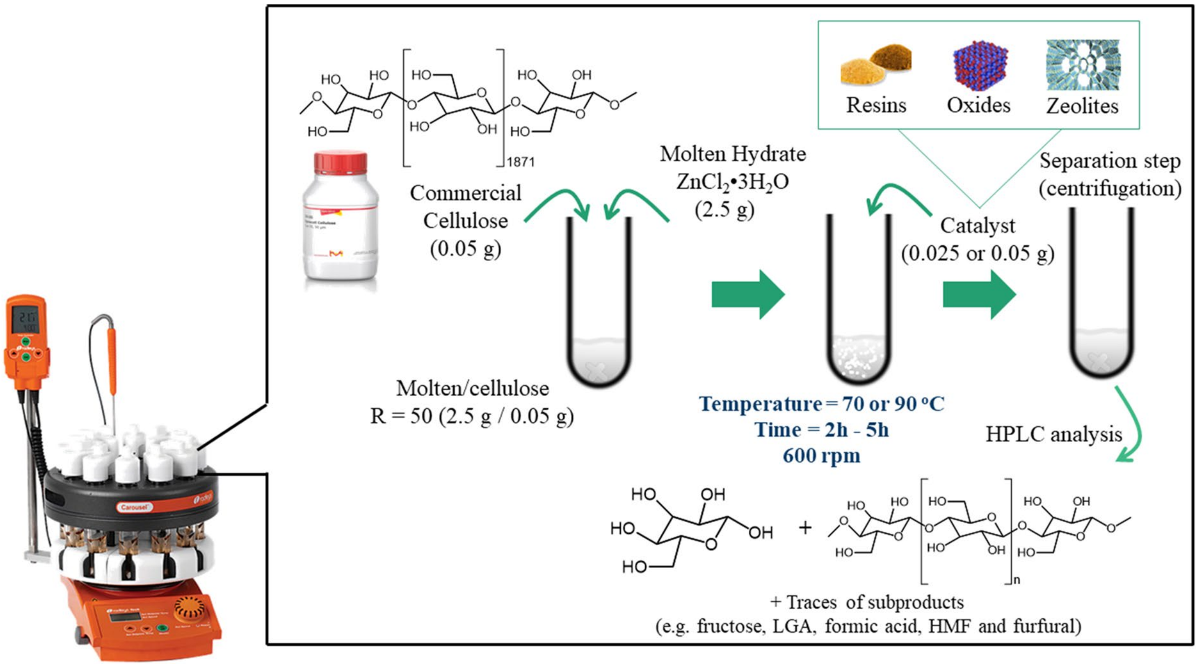

Fig. 1 Methodology applied for screening cellulose catalytic conversions

a 5 mmol L^{-1} H_2SO_4 solution as the mobile phase. Before HPLC analysis, the samples were filtered using a 0.22 µm Nylon filter. Products quantification was done according to calibration curves ($R^2 > 0.99$) prepared based on aqueous solutions of standards of the identified compounds. Products yields (Y) were determined by Eq. (1), where C_p and C_{cel_0} represent the mass concentration (g L^{-1}) of the product and the initial mass concentration of cellulose (g L^{-1}), respectively.

$$Y = \frac{C_P}{C_{cel_0}} \times 100\% \tag{1}$$

The content of oligomers was determined by a second hydrolysis step of the first produced hydrolysate, to obtain only monosaccharides, using a method developed by the US National Renewable Energy Laboratory (NREL) (Sluiter et al. 2008; Liu et al. 2019). In this case, 0.5 g of hydrolysate was mixed with a solution containing 2.5 g of 4 wt% H_2SO_4 in a reaction flask with a stirring bar. The flask was sealed and placed in a Radleys Carousel station previously heated to 130 °C and kept at this condition for 1 h under magnetic stirring (600 rpm). Then, the reaction flask was removed from the Radleys Carousel station and cooled down in a cold bath to room temperature. The resulting solution was analyzed by HPLC. In terms of quantification by Eq. 1, the difference between the final glucose yield obtained from this second step and that previously present in the initial hydrolysate provided the oligosaccharide yield of each reaction.

Catalyst stability tests

Catalyst stability (Fig. S1) was investigated by adding the same amount of catalyst used in the reactions (0.025 g or 0.05 g) to 2.5 g of zinc chloride salt solution in the H_2O/salt molar ratio of 3.0, in a reaction flask containing a stirring bar. The flask was sealed and placed in a Radleys Carousel station previously heated to 90 °C and kept at this temperature for 2 h under stirring (600 rpm). After this, the reaction flask was cooled down, the catalyst was removed by centrifugation. The supernatant solution was added to the reaction flask and 0.05 g of cellulose was introduced. The flask was, again, sealed and placed in the Radleys Carousel station still heated to 90 °C and kept at this condition for 2 h under stirring (600 rpm). Then, the reaction flask was removed from the Radleys Carousel station and cooled down and an aliquot of 0.3 g of the resulting hydrolysate was diluted 10 times for product analysis by HPLC.

The catalysts (oxides and zeolites) previously submitted to stability tests were then washed 4 times with deionized water, dried at 80 °C overnight, and analyzed by inductively coupled plasma optical emission spectroscopy in a 720-ES ICP-OES (Agilent) spectrometer with simultaneous CCD detection, in order to determine the elements (Al, Si, Nb, P, Zr, Zn) contents. Prior to the analysis, the samples were dissolved in 250 µL of HF, 4 mL of aqua regia (1 mL HNO_3 + 3 mL HCl), and heated to 110 °C for 2 h in the autodigestor Vulcan 42 (Questron). Then, the samples were neutralized by a solution containing triethanolamine (UniSolve—UNS1, Inorganic Ventures) and diluted up to 20 mL with ultrapure water.

For the ion-exchange polymer resins, elemental analysis (CHNS) was performed using a FlashSmart automated analyzer (Thermo Scientific) with a TCD (thermal conductivity) detector. Samples were weighted in tin containers and introduced into the combustion reactor. The reactor was filled with copper oxide followed by wire reduced nickel and maintained at 950 °C and operates with dynamic flash combustion of the sample. The resulting gases were separated on a packed column heated at 65 °C in an oven.

Catalyst reuse tests

To study the catalyst reuse, the most active spent catalysts in the first reaction cycle were recovered by centrifugation, washed 4 times with deionized water, dried at 80 °C overnight and thus used again in another catalytic test performed under the same conditions previously described. In addition, a regeneration step of some of the used catalysts (t-ZrO_2, $NbOPO_4$ and HZSM-5 $SiO_2/Al_2O_3 = 23$) by calcination at 400 °C for 2 h in an oven (under static air atmosphere) after washing process was also investigated.

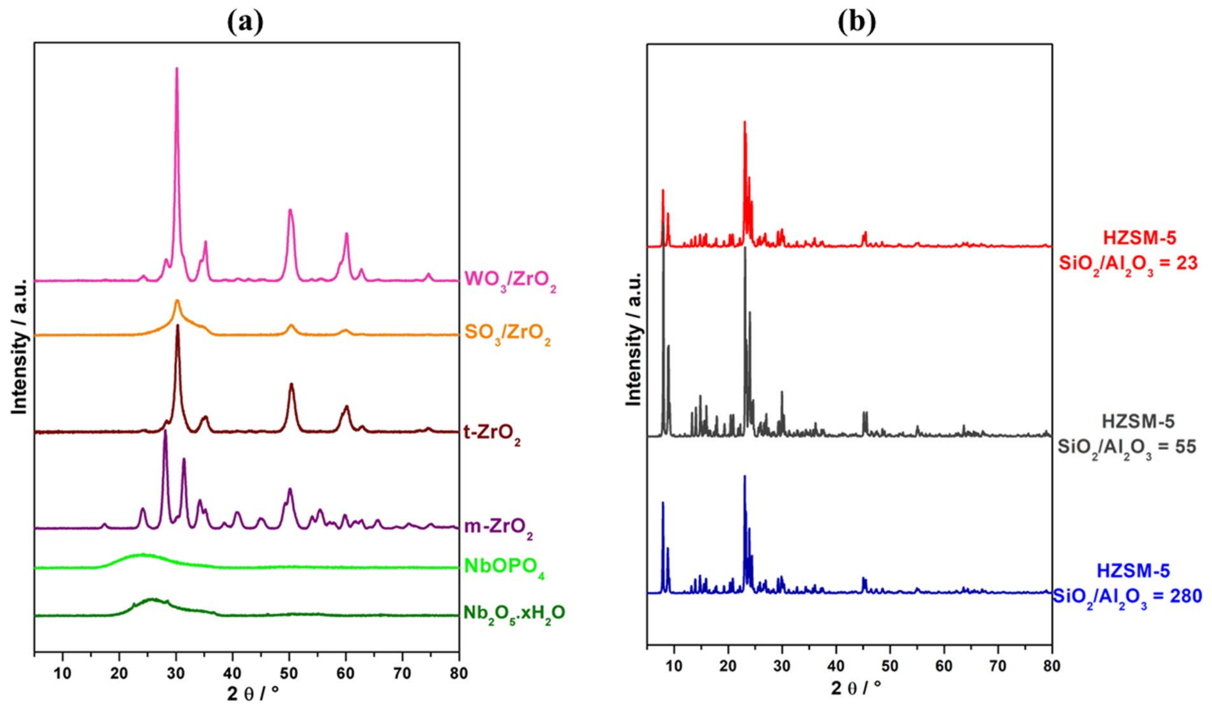

Fig. 2 XRD patterns obtained for: **a** metal oxides; and **b** HZSM-5 zeolites samples

Results and discussion

Catalysts characterization

Metal oxides and HZSM-5 catalysts were firstly characterized by XRD to identify their crystalline phases. Figure 2a, b show the diffractograms of metal oxides and HZSM-5 zeolite samples.

Both $Nb_2O_5 \cdot xH_2O$ and $NbOPO_4$ exhibited a diffractogram typical of a non-crystalline solid (de Souza et al. 2022), with only a broad line with a maximum around $2\theta = 25°$. ZrO_2 samples showed diffraction lines associated with monoclinic (m-ZrO_2, JCPD 37-1484) and tetragonal (t-ZrO_2, JCPD 17-0923) crystalline structures. ZrO_2 samples containing WO_3 and SO_3 groups presented only the lines characteristic of ZrO_2 with a tetragonal crystalline structure. The XRD patterns of HZSM-5 samples correspond to the MFI structure (JCPD 42-0024) reported in the literature (Sang et al. 2004; Ni et al. 2011).

Specific surface areas (S_{BET}) of the samples are summarized in Table 1. All metal oxides, except WO_3/ZrO_2, presented surface areas higher than 100 $m^2\ g^{-1}$. All HZSM-5 zeolites exhibited similar surface areas (401–432 $m^2\ g^{-1}$). Niobic acid ($Nb_2O_5 \cdot xH_2O$) and resins (Amberlyst-15, Dowex 50 and Dowex 650) did not have their textural properties (specific surface area and total pore volume) determined by this technique because the required thermal pretreatment for measurement could modify their structure and consequently change this property. The total pore volume of all the samples presented similar values, ranging from 0.13 to 0.3 $cm^3\ g^{-1}$, and among the oxides, $NbOPO_4$ showed the highest pore volume (0.3 $cm^3\ g^{-1}$).

The Brønsted acidity of the samples in the aqueous phase was evaluated by titration and the results are also reported in Table 1. Acid sites concentration varied from 21 to 6074 µmol g^{-1}. In comparison to the resins, the acidity of the solid catalysts was lower. Dowex 650 displayed the highest acidity among the three catalysts with Amberlyst-15 and Dowex 50 exhibiting similar acidity levels. Within the metal oxides, the acidity showed an increasing trend in the following order: $m\text{-}ZrO_2 < WO_3/ZrO_2 < Nb_2O_5 \cdot xH_2O < t\text{-}ZrO_2 < NbOPO_4 < SO_3/ZrO_2$. The concentration of acid sites of HZSM-5 samples decreased with the aluminum content in the zeolite

Table 1 Specific surface area (S_{BET}), total pore volume (V_p), Brønsted acidity measured by titration in an aqueous phase, and concentration of Lewis and Brønsted acid sites determined by Py-FTIR of the acid catalysts

Catalysts	S_{BET} ($m^2 g^{-1}$)	V_p ($cm^3 g^{-1}$)	Acidity (μmol g^{-1})				
			Aqueous titration	Py-FTIR			B:L ratio
				Brønsted (B)	Lewis (L)	Total	
Amberlyst-15	n.d	n.d	5223	n.d	n.d	n.d	n.d
Dowex 50	n.d	n.d	6074	n.d	n.d	n.d	n.d
Dowex 650	n.d	n.d	5308	n.d	n.d	n.d	n.d
WO_3/ZrO_2	85	0.19	106	15	64	79	0.2
SO_3/ZrO_2	151	0.24	605	65	142	207	0.5
t-ZrO_2	140	0.15	471	51	105	156	0.5
m-ZrO_2	139	0.13	21	0	117	117	0.0
$NbOPO_4$	122	0.30	538	26	87	113	0.3
$Nb_2O_5 \cdot xH_2O$	n.d	n.d	268	n.d	n.d	n.d	n.d
HZSM-5 $SiO_2/Al_2O_3 = 23$	418	0.21	668	603	150	753	4.0
HZSM-5 $SiO_2/Al_2O_3 = 55$	432	0.20	358	302	7	309	43.1
HZSM-5 $SiO_2/Al_2O_3 = 280$	401	0.19	152	128	1	129	128

n.d. not determined

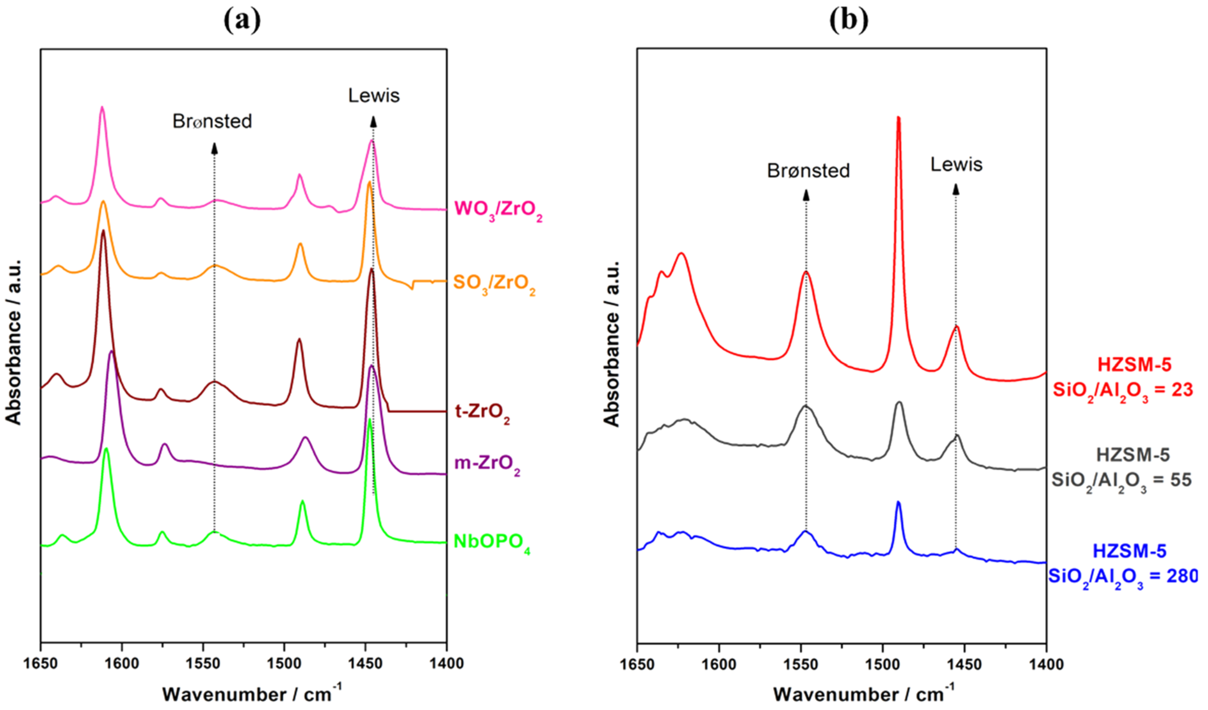

Fig. 3 Py-FTIR spectra obtained for: **a** metal oxides; and **b** HZSM-5 zeolite catalysts

framework. HZSM-5 $SiO_2/Al_2O_3 = 23$ showed the highest acidity (668 μmol g^{-1}).

The type of acid sites was determined by Py-FTIR and the obtained spectra are presented in Fig. 3a, b. In general, three bands were observed:

one located at 1442 cm^{-1} related to Lewis acid sites, other at 1542 cm^{-1} attributed to Brønsted acid sites and finally the band at 1490 cm^{-1} corresponding to a combination of these two types of sites. The concentration of Lewis and Brønsted acid sites are listed in Table 1. For the metal oxides catalysts, the highest concentrations of Brønsted acid sites were observed for SO_3/ZrO_2 and *t*-ZrO_2. In relation to Lewis acid sites, the acidity decreased in the following order $SO_3/ZrO_2 > m\text{-}ZrO_2 > t\text{-}ZrO_2 > NbOPO_4 > WO_3/ZrO_2$. For the HZSM-5 zeolites, the concentration of Brønsted acid sites determined by pyridine adsorption also decreases as SiO_2/Al_2O_3 ratio increases and they represent most of acid sites present on the zeolites.

Dissolution of cellulose in $ZnCl_2$ solutions

It is well known that molten salt hydrates such as $ZnCl_2$ are effective to promote cellulose dissolution, which can be affected by the cellulose degree of polymerization (D_p) and its crystallinity (Olsson and Westm 2013; Acharya et al. 2021). Therefore, dissolution tests were carried out to verify the efficiency of the $ZnCl_2$ in dissolving the Sigmacell cellulose ($D_p = 1871$) used in this work.

Cellulose dissolution was assessed by varying $H_2O/ZnCl_2$ molar ratios (R = 2.3, 3.0, 5.0 and 8.0) and using a molten salt/cellulose ratio of 50, as used in previous studies (Zhang et al. 2016; Wei and Wu 2017; Bodachivskyi et al. 2020). The cellulose dissolution was conducted at 70 °C for 1 h. Figure 4a, b show photographs of the solutions with different R. Cellulose is completely soluble in R = 3, since a transparent liquid was obtained. In the literature, the optimal $H_2O/ZnCl_2$ molar ratio (R) for cellulose dissolution has been reported to be in the between 3–4 (Sen et al. 2016; Awosusi et al. 2017; Wei and Wu 2017; Wang et al. 2020; Chen et al. 2020). For $H_2O/ZnCl_2$ molar ratio of 5.0 and 8.0, cellulose remained in suspension, while for the $H_2O/ZnCl_2$ molar ratio of 2.3, cellulose was partially dissolved, and a block of undissolved cellulose remained visible. This result does not agree with the literature that showed cellulose still in suspension at $H_2O/ZnCl_2$ ratio close to 2.3 (Sen et al. 2016). This might be attributed to the different temperature used in our work (70 °C) in comparison to the literature (25 or 50 °C).

The dissolution was also performed for 5 h and no significant changes were observed for $H_2O/ZnCl_2$

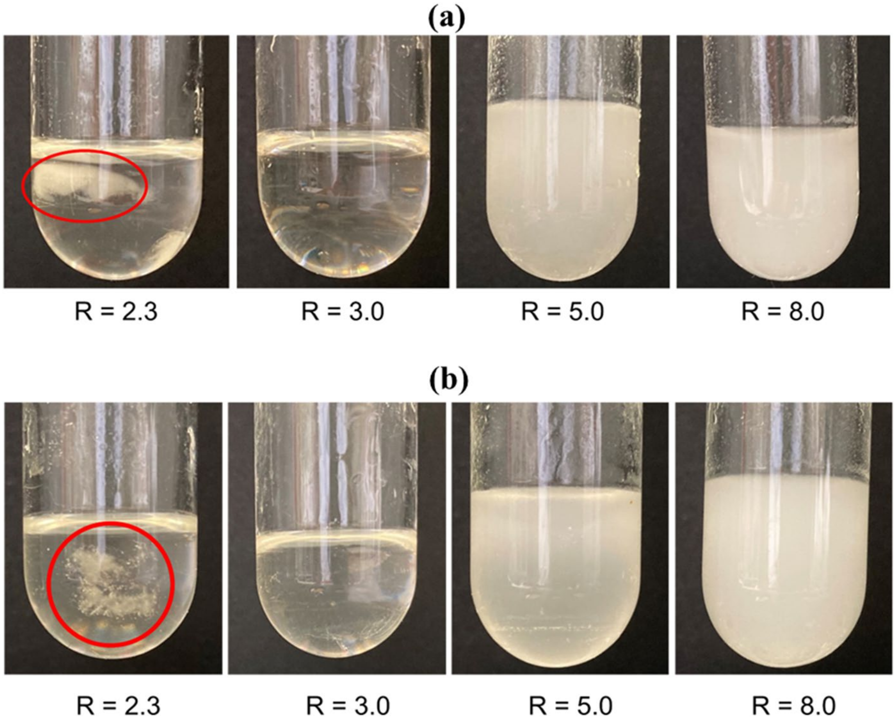

Fig. 4 Cellulose dissolution at 70 °C after **a** 1 h and **b** 5 h

molar ratios of 3.0, 5.0 and 8.0. On the other hand, for the $H_2O/ZnCl_2$ molar ratio of 2.3, the amount of dissolved cellulose increased but, even so, cellulose was not completely dissolved since it is still possible to observe some cellulose particles suspended in the solution (Fig. 4b).

Depolymerization of cellulose using $ZnCl_2$ R = 3.0

The solubilization of cellulose with MSH may be accompanied by its depolymerization and hydrolysis. The conversion of cellulose and product distribution depends on the type of inorganic molten salt, the MSH/cellulose molar ratio, reaction temperature, and time (Wei and Wu 2017; Liu et al. 2019, 2021a, b, 2022; Wang et al. 2020). Initially, experiments were conducted at temperatures of 70 and 90 °C with varying reaction times, using the previously determined optimal $H_2O/ZnCl_2$ molar ratio of 3.0 for cellulose solubilization, and without the presence of a catalyst.

At 70 °C after 5 h, no glucose formation was observed under these reaction conditions. In fact, unreacted cellulose was detected after sample dilution, and the amount of recovered cellulose matched the initial quantity used at the beginning of the reaction. This result reveals that no cellulose was converted without the presence of a catalyst at this temperature.

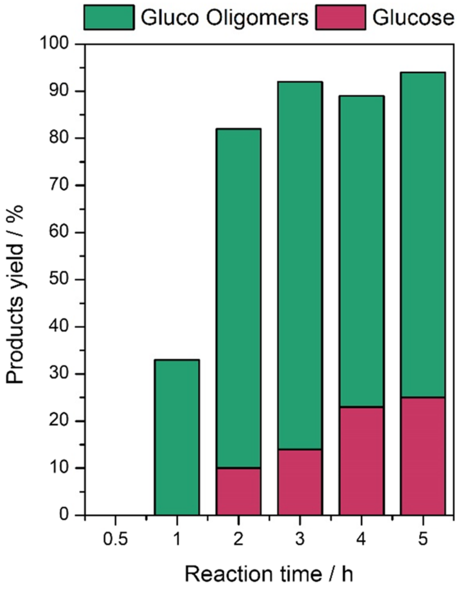

Fig. 5 Products yield obtained by the depolymerization of cellulose using $ZnCl_2$ with a H_2O/molten salt hydrate molar ratio of 3.0 at different reaction times. Reaction conditions: T = 90 °C, 2.5 g of $ZnCl_2$ R = 3.0, 0.05 g of cellulose

Figure 5 shows the product yield obtained by the depolymerization of cellulose at 90 °C using $ZnCl_2$ with a H_2O/molten salt hydrate molar ratio of 3.0 at different reaction times. As the reaction temperature was increased to 90 °C, glucose remained undetected and unreacted cellulose was recovered from the solution after 0.5 and 1 h of reaction. The amount of unreacted cellulose recovered after 0.5 and 1 h of reaction corresponded to 100% and 67% of the initial cellulose, respectively, demonstrating that cellulose depolymerization by the MSH occurred after 1.0 h of reaction at 90 °C. However, despite partial depolymerization of cellulose, no glucose or its derived products were observed on the HPLC, producing only gluco oligomers that are not detected in our column. After 2 h of reaction, no cellulose in suspension was observed in the aliquots following sample dilution with H_2O, indicating that cellulose was completely depolymerized (100% of conversion). However, only a small amount of glucose was detected in the samples (10% yield). Increasing the reaction time to 3 h, the glucose yield only slightly increased to 15%. The maximum yield of glucose was achieved after 5 h of reaction (25%). These results suggest that cellulose was primarily converted into gluco oligomers that further reacted to glucose. To validate this observation, a second hydrolysis reaction was performed on the hydrolysate collected from 1 h onward, using H_2SO_4 (4%), and the amount of gluco oligomers was estimated by the yield of glucose obtained after the second hydrolysis reaction. As shown in Fig. 5, glucose and gluco oligomers were the main products formed. Increasing the reaction time enhanced the glucose yield, while the formation of oligomers decreased. Despite the complete conversion of cellulose, the sum of the total product yield (gluco oligomers and glucose) remained around 90%. In fact, the orange color of the solution after 4 and 5 h of reaction suggests that humins were formed (Fig. S2), which may explain the carbon balance of around 90%.

Cellulose conversion in the presence of MSH without catalyst has been reported in the literature (Zhang et al. 2016; Wei and Wu 2017; Wang et al. 2020; Ma et al. 2022a, b), however, the temperatures employed in those experiments were higher (120–190 °C) compared to the one used in this study (90 °C). Therefore,

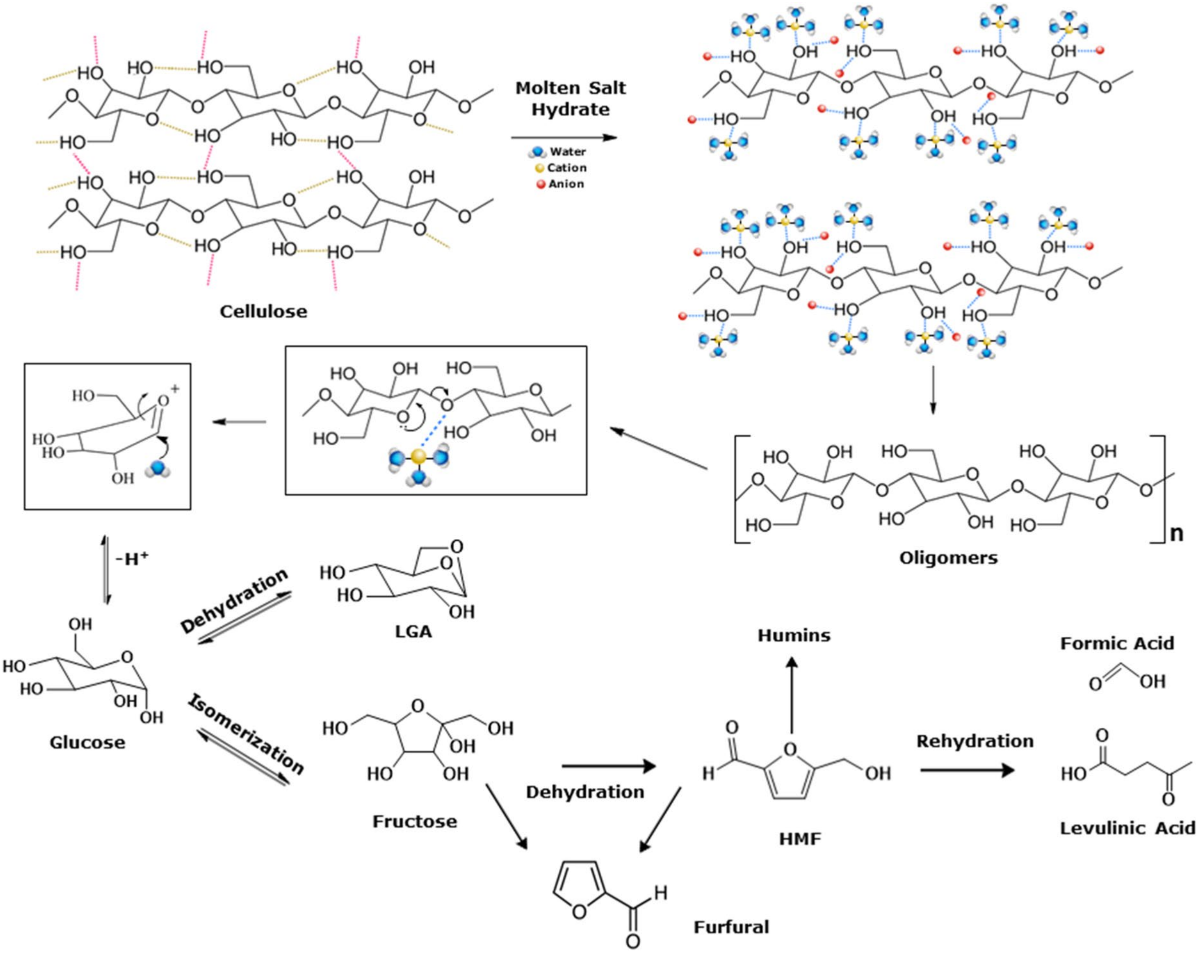

Scheme 1 Proposed reaction mechanism and products in MSH (Paiva et al. 2024)

products from glucose conversion such as HMF and LA have also been observed under high temperatures. Ma et al. (2022a, b) investigated the conversion of cellulose with different MSH without catalyst in a biphasic system at 180 °C for 20 min. Unreacted cellulose and gluco oligomers were obtained with LiI, NaCl, NaBr, NaI, KCl, KI, whereas only unreacted cellulose was observed for $ZnCl_2$, even at the high temperature used. Wang et al. (2020) observed a high yield to LA when the conversion of cellulose was carried out with $ZnCl_2$, but a significant formation of humins also occurred due to the high reaction temperature used (175 °C). These results demonstrate that temperature limits the hydrolysis rate of cellulose in the presence of MSH. Quiroz et al. (Rodriguez Quiroz et al. 2019a) highlighted that the hydrolysis rate of cellulose by MSH is slow at low reaction temperatures due to its lower acidity in comparison to concentrated acid solutions. To prove this, we conducted a test with cellobiose, a cellulose surrogate molecule, with $ZnCl_2$ and without catalyst at 90 °C. The product yields obtained in the depolymerization of cellobiose using $ZnCl_2$ with a H_2O/molten salt hydrate molar ratio of 3.0 are shown in Fig. S3. Glucose was the main product formed (61%), but now, significant amounts of fructose (2%), LGA (6%) and HMF (1.6%) were also detected. Therefore, the MSH breaks intra- and inter-molecular hydrogen bonds in the cellulose structure, producing gluco oligomers (e.g., cellobiose, cellotriose, cellotetrose and cellopentose) (Sadula et al. 2017) that can then be converted into glucose. In the presence of an acid or high temperature, glucose can undergo two

Fig. 6 Products yield observed after reaction **a** at 70 °C after 5 h and **b** at 90 °C after 2 h. Reaction conditions: 2.5 g of $ZnCl_2$ R = 3.0, 0.05 g of cellulose and 0.025 g of catalyst

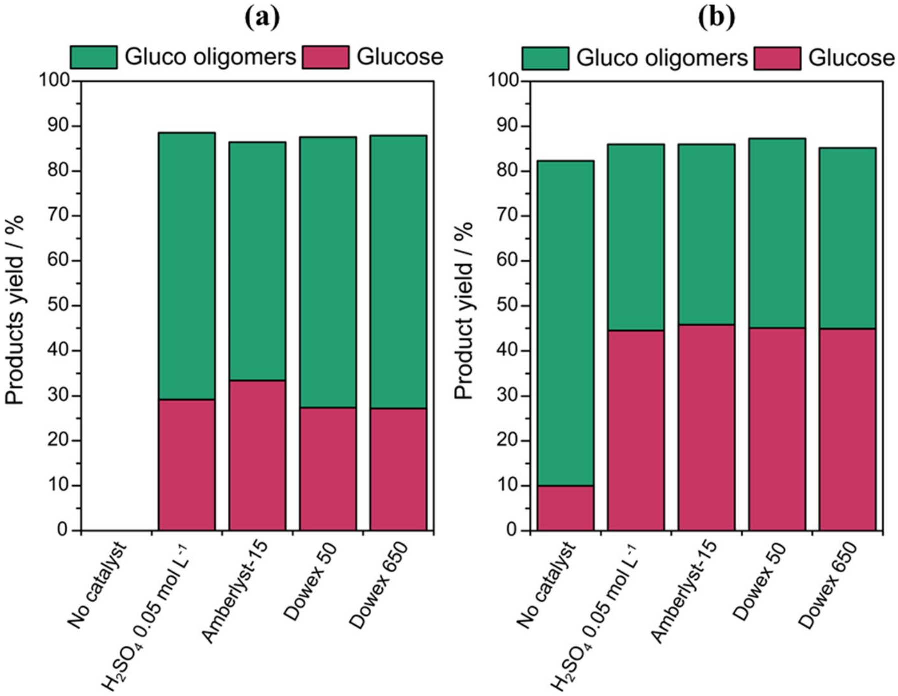

distinct reaction pathways: (i) dehydration to LGA; (ii) isomerization to fructose in the presence of Lewis acids, which can be further dehydrated to HMF catalyzed by Brønsted acids. Then, the hydration of HMF produces levulinic acid and formic acid or HMF can undergo polymerization with sugars resulting in the formation of humins (Scheme 1) (Paiva et al. 2024).

Depolymerization of cellulose using $ZnCl_2$ R = 3.0 in the presence of solid acid catalysts

In this work, three series of solid acid catalysts with different acid properties were evaluated for the hydrolysis of cellulose using $ZnCl_2$ with R = 3.0: Ion-exchange polymer resins, metal oxides and zeolites. Some of these catalysts exhibit only strong Brønsted acidity ($–SO_3H$ based polymers), whereas the metal oxides and zeolites contain both Brønsted and Lewis acid sites, but with different ratios (Table 1). Metal oxides have a lower B/L ratio between 0 and 0.5 whereas zeolites possess much higher B/L ratio (4–128). Next, we will discuss the performance of each series of catalysts.

Ion-exchange polymer resins (Amberlys-15, Dowex 50 and Dowex 650) contain sulfonic groups ($–SO_3H$) that are strong Brønsted acid sites. Initially, the resins were evaluated at 70 °C for 5 h (Fig. 6a) to investigate the effect of the catalyst on the depolymerization of cellulose, since no conversion of cellulose occurred without catalyst at this temperature, as previously discussed. Test was also performed with H_2SO_4, which is a common inorganic acid used in cellulose hydrolysis studies. The concentration of H_2SO_4 (0.05 mol L^{-1}) employed in the reaction corresponded to the same amount of H^+ present in all three resins as indicated by their manufacturer, and it corresponds to the concentration generally present on homogeneous studies in the literature.

Figure 6a shows the products yield obtained after reaction at 70 °C. Both glucose and gluco oligomers were formed, regardless of the catalyst used. In the presence of H_2SO_4, the glucose yield reached approximately 30%. The three resins exhibited similar performance with the glucose yield between 27 and 33%, while the oligomer content was around 60%. In fact, the amount of H^+ indicated by the manufacturer for the resins are close (1.7 meq mL^{-1} for Amberlyst-15 and Dowex 50 and 2.0 meq mL^{-1} for Dowex 650, in a wet basis), which justify the similar results obtained. The acidity of these resins was also assessed by titration (Table 1) and even though Dowex 650 presented higher concentration of acid sites, its behavior was the same as the other samples. Therefore, the solid acid catalysts exhibited the same activity than the homogeneous catalyst but with the advantage that they can be recovered and reused in the process.

As noted in previous experiments using only the MSH, glucose was already detected after 2 h of reaction at 90 °C. Therefore, these reaction conditions were chosen to assess the performance of the resins with the aim at enhancing glucose yield and shortening the reaction duration. The product yield obtained after reaction at 90 °C without any catalyst and in the presence of H_2SO_4 and resins are shown in Fig. 6b. At 90 °C, the conversion of cellulose is observed even without catalyst, producing 10% of glucose and 72% of gluco-oligomers. Increasing the reaction temperature to 90 °C significantly improved the glucose yield to around 45% for all resins as well as for H_2SO_4. This demonstrates that combining the high acidity of resins with the higher temperature (90 °C) was beneficial. However, resins such as Amberlyst-15 and Dowex 650 exhibit stability only at temperatures up to 120 and 150 °C, respectively, limiting the possibility of further increasing the reaction temperature.

Tests at different reaction times and 90 °C using Amberlyst-15 resin were also performed and the products yields obtained are displayed in Fig. 7. The yields of glucose and oligomers remained constant until 4 h. Then, a reduction in glucose and gluco oligomers yields is observed. This result is primarily attributed to the formation of insoluble degradation products (humins), leading to the darkening of the hydrolyzed solution.

Commercial metal oxides ($Nb_2O_5 \cdot xH_2O$, $NbOPO_4$, *m*-ZrO_2, *t*-ZrO_2, SO_3/ZrO_2 and WO_3/ZrO_2) were also evaluated for the cellulose hydrolysis with $ZnCl_2$ R = 3.0 at 90 °C for 2 h and the results are shown in Fig. 8.

Initially, experiments were done using the same mass of metal oxide as used in the reaction performed with the resins (0.025 g). However, the glucose yield obtained was the same as in the experiment containing only the molten salt hydrate and thus, the catalyst mass was doubled, to observe the influence of the catalytic system and in an intent to increase glucose yield. As presented in Fig. 8, gluco oligomers were the main products formed for all catalysts, while the glucose yield varied between 11 and 27%. Trace amounts of fructose, levoglucosan, HMF and furfural were detected but below the quantification limit. Even

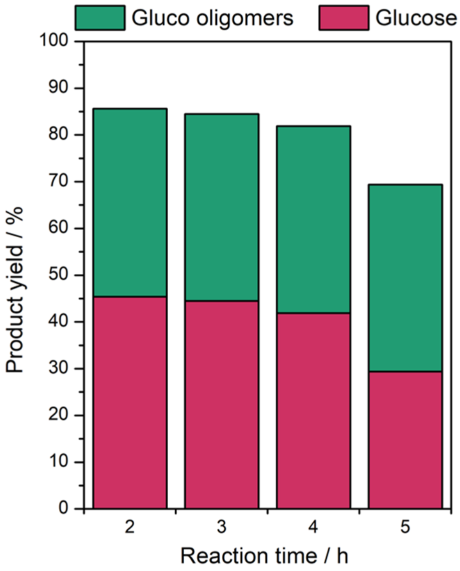

Fig. 7 Products yield obtained by the depolymerization of cellulose using Amberlyst-15 as catalyst at different reaction time. Reaction conditions: T = 90 °C, 2.5 g of $ZnCl_2$ R = 3.0, 0.05 g of cellulose and 0.025 g of catalyst

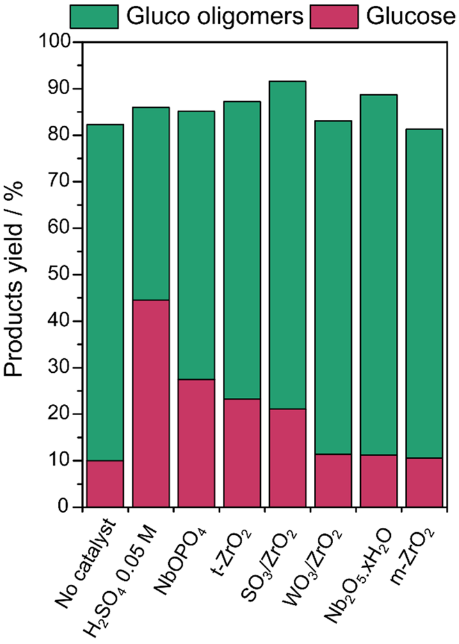

Fig. 8 Products yield obtained by the depolymerization of cellulose using different metal oxides. Reaction conditions: T = 90 °C, 2.5 g of $ZnCl_2$ R = 3.0, 0.05 g of cellulose and 0.05 g of catalyst

though the oxides exhibited glucose yield lower than that for the resins or homogeneous system with sulfuric acid solution, it was still higher than without catalyst, except for $Nb_2O_5.xH_2O$, *m*-ZrO_2 and WO_3/ZrO_2 that showed glucose yield close to the one observed when only $ZnCl_2$ R = 3.0 was used. The highest glucose yield observed for $NbOPO_4$, *t*-ZrO_2 and SO_3/ZrO_2 can be attributed to their higher levels of Brønsted acidity as indicated in Table 1. While the specific Brønsted acid sites of $Nb_2O_5.xH_2O$ were not quantified, its comparatively lower performance suggests that it possesses a lower concentration of Brønsted acid sites in comparison to $NbOPO_4$, *t*-ZrO_2 and SO_3/ZrO_2, and is closer in acidity to WO_3/ZrO_2.

Metal oxides such as $NbOPO_4$, *t*-ZrO_2 and SO_3/ZrO_2 have demonstrated their potential as catalysts for the cellulose hydrolysis. They effectively cleaved gluco oligomers, yielding glucose at levels comparable to those achieved with MSH at significantly lower temperature. The difference between the observed activity of these catalysts in relation of the expected acidity scale (Table 1) is due to specific distribution and strength of acid sites.

The obtained glucose yields were lower than those reported by Wei and Wu (2017), using SO_4/TiO_2 under similar reaction conditions (90 °C, $ZnCl_2$/cellulose ratio = 50 and catalyst/cellulose ratio = 1). However, it is important to note that the cellulose used here has a higher degree of polymerization ($D_p = 1871$) than the other commercial celluloses generally used in the literature (e.g. Avicel PH-101 $D_p = 241$, Sinopharm Type50 $D_p = 246$ and Aladdin MCC250 $D_p = 220$) (Zhang et al. 2014) and that the reaction time of 2 h was shorter than that used by the authors (3 h). Furthermore, evaluating the acidic properties obtained by pyridine adsorption infrared spectra, the SO_4/TiO_2 catalyst is much more acidic (Brønsted = 728.3 $\mu mol\ g^{-1}$, Lewis = 302.2 $\mu mol\ g^{-1}$ and B:L = 2.41), than the oxides presented in this work (Table 1).

Zeolites, characterized by their abundant Brønsted acid sites, are preferred solid acid catalysts, particularly in processes dependent on these acid sites, such as hydrolysis reaction. In this work, HZSM-5 zeolite with three different SiO_2/Al_2O_3 ratio were tested in the presence of $ZnCl_2$ R = 3.0 at 90 °C and the results are depicted in Fig. 9. For comparative purposes, this figure also shows the case where only the MSH was added (without catalyst), and with the homogenous catalyst (H_2SO_4) at the same H^+ concentration as observed for the HZSM-5 with a $SiO_2/Al_2O_3 = 23$ (the most acid zeolite).

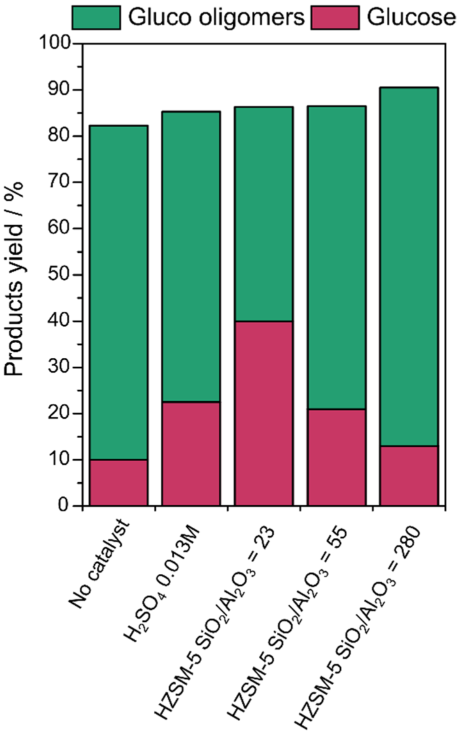

Fig. 9 Products yield obtained by the depolymerization of cellulose using HZSM-5 zeolites with different SiO_2/Al_2O_3 ratio. Reaction conditions: T = 90 °C, 2.5 g of $ZnCl_2$ R = 3.0, 0.05 g of cellulose and 0.05 g of catalyst

All HZSM-5 zeolites were very active, promoting the gluco oligomers hydrolysis and producing glucose yields ranging from 16 to 40%. Glucose yield decreased as SiO_2/Al_2O_3 ratio increased, which is likely due to the lower content of Al in the zeolite framework that leads to lower acidity, as shown in Table 1.

HZSM-5 $SiO_2/Al_2O_3 = 23$ demonstrated to be a promising catalyst since it presented glucose yields higher than H_2SO_4 (two-fold) and showed a comparable performance to the resins. Also, if compared to the metal oxides, its activity was higher than the three most active oxide catalysts.

The conversion of cellulose using MSH in the presence of diluted acid, the so-called acidic molten salt hydrate (AMSH), has been studied in the literature (de Almeida et al. 2010; Deng et al. 2012, 2015; Zhang et al. 2017; Wei and Wu 2017; Liang et al.

Table 2 Cellulose conversion in molten salt hydrates solutions

Substrate	MSH	Catalyst	Reaction conditions	Main products (% yield)	References
Cellulose	LiBr	H_2SO_4 (0.05 M)	85 °C, 30 min	Glucose (78%) dimers (12%)	Deng et al. (2015)
Cellulose	$ZnCl_2$ (63 wt%)	HCl	120 °C	HMF (30%)	Deng et al. (2012)
Microcrystalline cellulose	$ZnCl_2$ (72 wt%)	HCl (0.2 M)	150 °C	HMF (69.5%)	Zhang et al. (2017)
Cellulose	$ZnCl_2$ (70 wt%)	HCl (0.4 M)	85 °C	Glucose (98%)	de Almeida et al. (2010)
Cellulose	$ZnCl_2·3H_2O$	SO_4/TiO_2	90 °C	Gluco oligomers (9.4%) glucose (50.5%) fructose (5.9%) HMF (3.4%) LA (5.1%)	Wei and Wu (2017)
Microcrystalline cellulose	LiBr (60 wt%)	Beta and ZSM-5 zeolites with $SiO_2/Al_2O_3=30$ and 50	120 °C, 0.5 h	Gluco oligomers (54.4%) glucose (28.3%) HMF (0.2%)	Wu et al. (2020)
Microcrystalline cellulose	$LiCl·3H_2O$	Nb_2O_5, $NbOPO_4$, HZSM-5, $NbOPO_4$/HZSM-5	175 °C, 2.0 h, biphasic system	LA (85.1%) HMF (5%)	Wang et al. (2020)
Microcrystalline cellulose	LiBr (55 wt%)	Activated carbon	110 °C, 2.0 h	Glucose (80%) LA (4%)	Liang et al. (2022)

2022). Table 2 lists the yields of different products obtained for the conversion of cellulose with various AMSH. Different MSH, reaction conditions (temperature, time, acid type and concentration) and processes (one or two-steps, biphasic solvent) have been used, which makes difficult a comparison with our work. Comparing the results obtained with inorganic acid (H_2SO_4) of our work with the literature, it seems that a higher glucose yield was obtained using LiBr as MSH at 85 °C (Deng et al. 2015). At higher temperatures, a high yield to HMF was observed in the presence of $ZnCl_2$, but a biphasic solvent was required to reduce the formation of humins (Deng et al. 2012; Zhang et al. 2017).

The glucose yield obtained at 90 °C and 2 h using HZSM-5 $SiO_2/Al_2O_3=23$ is slightly lower than that reported in the literature over SO_4/TiO_2 catalyst. However, a higher formation of oligomers was produced with our catalyst. The conversion of cellulose using LiBr was carried out at higher temperatures over Beta and ZSM-5 zeolites (120 °C) and activated carbon (110 °C), resulting in the formation of 28 and 80% of glucose, respectively. These differences in glucose yield at approximately the same temperature could be attributed to differences in acidity of the catalysts. When the reaction was performed at higher temperature (175 °C) over Nb_2O_5; $NbOPO_4$; HZSM-5; $NbOPO_4$/HZSM-5 catalysts, a significant formation of LA was achieved, but a solvent was added to control the formation of humins.

An experiment with cellobiose was also performed using HZSM-5 $SiO_2/Al_2O_3=23$ at 90 °C and 2 h (Fig. S3). Complete conversion of cellobiose was achieved, producing mainly glucose (68%) but also fructose (4%), LGA (6.7%), HMF (5%), furfural (4%) and formic acid (8.6%). Therefore, the absence of formation of products other than glucose is due to limitation in the rate of cellulose hydrolysis at this low reaction temperature (90 °C).

Catalyst stability and reusability

One of the advantages of heterogeneous catalysts is the possibility of recovering and reusing the catalyst. Then, the heterogeneous catalyst must present high chemical stability and must be resistant to deactivation. Considering that the pH of the $ZnCl_2$ $R=3.0$ solution is very low (<1), it can affect the catalyst chemical composition. Therefore, catalysts stability in the acid solution of MSH was evaluated for the most active catalysts. In this test, the catalysts were maintained in the presence of $ZnCl_2$ $R = 3.0$ solution (90 °C, 2 h). Next, the catalysts were removed from the solution, in which cellulose was added and remained for 2 h. The glucose yield above that observed for the test without catalyst (10%, as present in Figs. 8 and 9) indicates that the catalyst lost part of its active sites (Lewis and

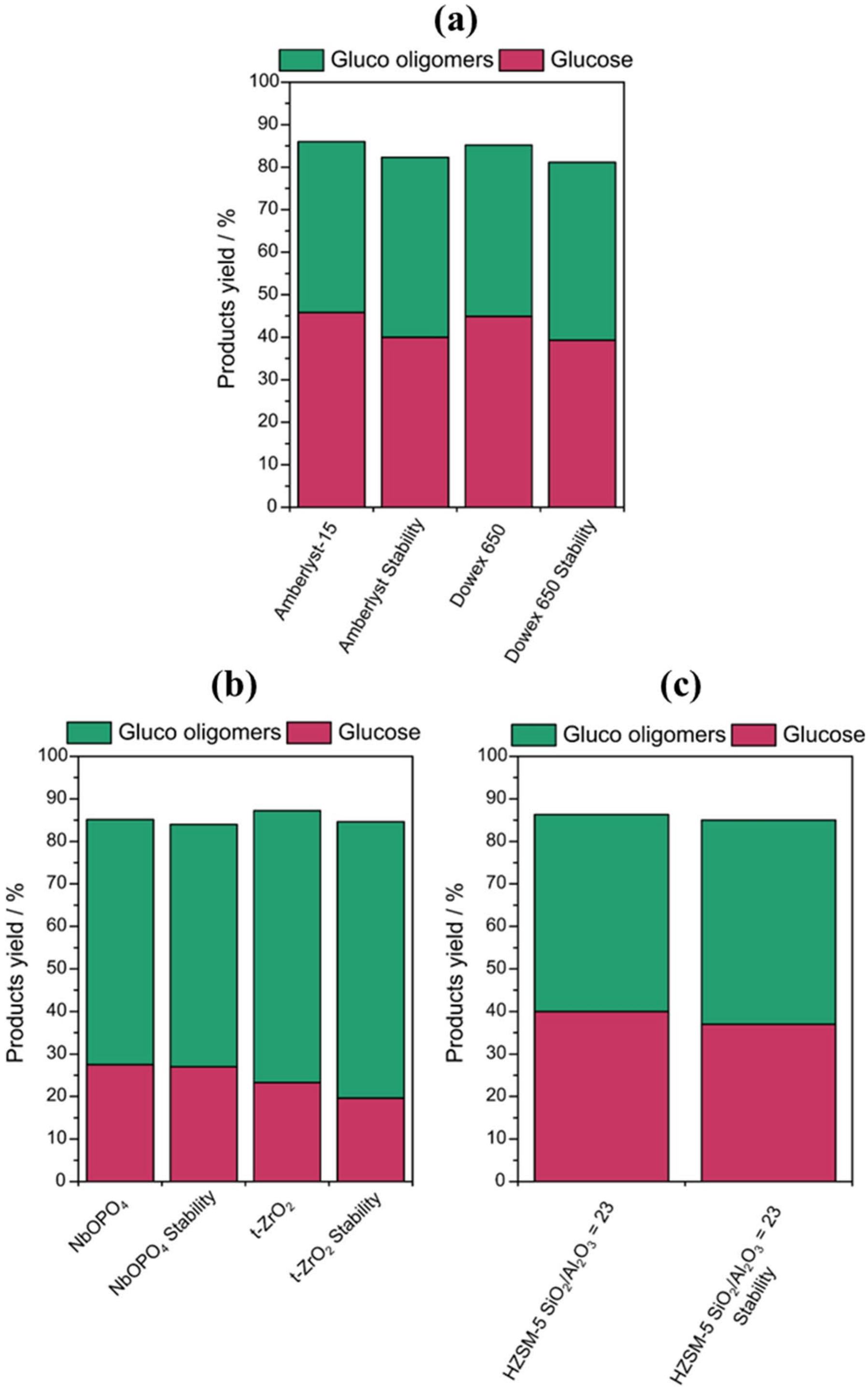

Fig. 10 Glucose yield observed after the stability tests for **a** resins catalysts, **b** metal oxides catalysts, and **c** zeolite catalyst

Brønsted acid sites) when in contact with the MSH. On the other hand, the same glucose yield than that for the test without catalyst shows that catalyst remained stable.

Figure 10 shows the glucose yield obtained after the stability tests for (a) resins; (b) metal oxides and (c) zeolites catalysts. For Amberlyst-15 and Dowex 650 resins, the glucose yield achieved was 44%, indicating that both resins do not maintain their stability under the reaction conditions.

Since $NbOPO_4$ and t-ZrO_2 exhibited the highest yield of glucose among the studied metal oxide catalysts in this work, their stability was also evaluated in the same way used for the resins. These catalysts also presented high glucose yields after the stability tests, indicating that they also are not stable either (Fig. 10b). Furthermore, it was observed a reduction around 40% wt.% in relation of the initial catalyst amount used for the tests, indicating the occurrence of dissolution of the metal oxides after the first reaction cycle.

As it was observed for other tested catalysts, HZSM-5 $SiO_2/Al_2O_3=23$ was also affected by the reaction conditions used in this work, showing a glucose yield around 37% after the stability tests (Fig. 10c).

The stability results revealed that none of the top-performing catalysts retained their initial properties after the reaction. This suggests that these materials may have been affected by the reaction conditions applied in the experiments. Notably, the high acidity of the $ZnCl_2$ molten salt hydrate solution can induce deactivation processes, primarily involving leaching of the functional groups from the resins, dissolution in the case of the metal oxides, or by ion exchange in the zeolites. Thus, additional experiments were carried out in order to characterize the spent catalysts and to contribute to a better comprehension of the deactivation mechanisms occurring during the reaction.

Table 3 Elemental analysis (CHNS) of resin before and after stability test

Catalysts	Elements contents (wt.%)		
	C	H	S
Amberlyst-15	44.1 ± 0.1	5.0 ± 0.02	14.4 ± 0.8
Amberlyst-15 after use in $ZnCl_2$ R = 3.0	38.5 ± 0.5	4.4 ± 0.1	12.4 ± 0.4

In the case of the ion exchange resin Amberlyst-15, elemental analysis via CHNS (Table 3) performed before and after the stability experiment revealed a reduction of 12–14% in the amount of the elements present in the solid (C, H, and S). This confirms the leaching of this catalyst, with the removal of sulfonic groups (SO_3H), induced by the strong acidity of the reaction medium and the conditions used, which can favor the breaking of bonds in the polymeric structure of the resin and consequent loss of active sites.

For the oxides (Table 4), ICP-OES analysis revealed reductions in the percentage of the elements analyzed, mainly due to the presence of traces of Zn in the used catalysts. This suggests that ion exchange can occurs between the solids and the reaction media, where for every $2H^+$ released by the catalyst into the solution, one cation Zn^{2+} is ionically exchanged on the solid. This process can potentially reduce catalyst activity in subsequent hydrolysis reactions, as it reduces the Brønsted acidity while increasing the Lewis acidity of the system. Furthermore, in the case of $NbOPO_4$, the observed reduction for P content confirm that the exposure of the heterogeneous catalysts to the $ZnCl_2$ medium with R = 3.0 promoted dissolution and leaching of elements.

An ICP-OES analysis was also conducted on the HZMS-5 zeolite ($SiO_2/Al_2O_3=23$). After the reaction in the presence of the MSH, desilication and dealumination were detected, leading to structural modifications and a subsequent alteration in the original Si/Al ratio of the zeolite (Table 5), which

Table 4 Elemental analysis (ICP-OES) of oxides samples before and after the stability test

Catalysts	Elements contents (wt.%)			
	Nb	P	Zr	Zn
$NbOPO_4$	45.6 ± 1.2	15.2 ± 0.5	0.0	0.0
$NbOPO_4$ after use in $ZnCl_2$ R = 3.0	30.9 ± 0.1	11.5 ± 0.07	0.0	2.41 ± 0.01
t-ZrO_2	0.0	0.0	49.8 ± 0.3	0.0
t-ZrO_2 after use in $ZnCl_2$ R = 3.0	0.0	0.0	36.7 ± 0.2	0.320 ± 0.01

Table 5 Elemental analysis (ICP-OES) of zeolite sample before and after stability test

Catalysts	Elements contents (wt.%)			
	Si	Al	Zn	Si/Al (molar ratio)
HZSM-5 $SiO_2/Al_2O_3 = 23$	35.9 ± 0.2	2.9 ± 0.02	0.0	11.6 ± 0.1
HZSM-5 $SiO_2/Al_2O_3 = 23$ after use in $ZnCl_2$ R = 3.0	32.7 ± 0.1	2.3 ± 0.02	2.6 ± 0.01	13.4 ± 0.06

increased to 13.4. This indicates a reduction in the acidity of the catalyst after use, as a higher silicon/aluminum molar ratio indicates fewer compensating cations and lower Brønsted acidity. Additionally, considering that the molar quantity of aluminum (2.9 wt.% $= 1.07 \times 10^{-5}$ mol of Al) initially present in the zeolite is equimolar to the protons available for the reaction (Giannetto Pace 2000), and evaluating the amount of Zn present in the zeolite after use, it was noticed that 74.2% of all the protons available in the zeolitic catalyst were ion exchanged with this cation (Zn^{2+}). This elucidates the deactivation after the first reaction cycle, following a homogeneous ion exchange mechanism, a result consistent with a previous work described in the literature (Wu et al. 2020).

Therefore, the high acidity of the $ZnCl_2$ molten salt hydrate solution can induce deactivation processes, primarily involving leaching of the functional groups from the resins, dissolution in the case of the metal oxides, or by ion exchange in the metal oxides and zeolites.

Even with these results, attempts were made to reuse the t-ZrO_2, $NbOPO_4$, and HZSM-5 $SiO_2/Al_2O_3 = 23$ catalysts after the first cycle, for which the used catalysts were washed (4 times in ultrapure water) and dried (80 °C) overnight. A series of reactions using the same catalysts were made to accumulate sufficient mass to be able to perform a new reaction cycle with the used catalyst at the same amount of fresh catalysts. All three catalysts exhibited the same glucose yield obtained in the experiment using only $ZnCl_2$ R = 3.0 medium (10% of glucose yield), confirming that catalysts deactivated after the first reaction. A further test was performed, but this time, the catalysts used in the first cycle were washed, dried, and then, they were treated under air at 400 °C 2 h, in order to remove any carbon deposits from the previous reaction that might be present, and which could also block the active sites. Again, even having adopted this previous treatment step, the results obtained were equivalent to the system employing only $ZnCl_2$ R = 3.0, indicating that this treatment was not enough to regenerate the catalyst. Therefore, additional treatments such as a new ion exchange are required to regenerate the properties of these solid catalysts.

Conclusions

The use of zinc chloride molten salt hydrate ($ZnCl_2 \cdot 3.0H_2O$) in the presence of commercial resins, metal oxides, and zeolites as catalysts made it possible not only to solubilize cellulose but also to promote its simultaneous depolymerization and conversion to oligomers and glucose under mild conditions. The presence of these catalysts selectively increased the production of glucose when compared to the reaction with the MSH alone, which produced more oligomers. Moreover, in the case of HZSM-5 $SiO_2/Al_2O_3 = 23$, higher products yield than the traditional homogeneous system using H_2SO_4 at the same acid site concentration was obtained. Unfortunately, solid catalysts exhibited instability in the presence of MSH, likely due to the extremely low pH of the solution. This instability led to catalyst deactivation, primarily through processes such as the leaching of functional groups from the resins, dissolution in the case of metal oxides, or ion exchange in the zeolites. Despite efforts, including washing, drying, and calcination processes to promote the reuse of the best spent catalysts, they exhibited the same glucose yield as the $ZnCl_2$ R = 3.0 blank experiment. This result confirmed that the catalysts lost their activity after the first reaction and that additional treatments such as a new ion exchange are required to regenerate the properties of these solid catalysts.

Acknowledgments The authors acknowledge Region Hauts-de-France for “CatBioInnov” project, the Ministère de l’Enseignement Supérieur et de la Recherche and the European Regional Economic Development Fund for their financial support to the CPER ECRIN program. Mateus Freitas Paiva acknowledges the Program for Early stage in Lille (Pearl, No. 8475-68) and Elise Mota Albuquerque thanks the Make our Planet Again (MOPGA) program (mopga-postdoc-3-7957230435).

Author contributions All authors participated in the conceptualization and design of the study. Material preparation, data collection, and analysis were performed by E. M. Albuquerque, M. F. Paiva, and P. M. de Souza. The first draft of the manuscript was written by M. F. Paiva and E. M. Albuquerque. Funding acquisition was coordinated by F. B. Noronha, R. Wojcieszak, G. Vanhove, and J. H. Bitter. All authors assisted equally in article manuscript revision, commenting on versions and in discussion of the results. All authors have read and agreed to the published version of the manuscript.

Funding This study was supported by the Programme Investissement d’Avenir (I-SITE ULNE/ANR-16-IDEX-0004 ULNE). CNRS, Métropole Européen de Lille (MEL), European Union’s Horizon 2020 Research and Innovation Programme (Marie Skłodowska-Curie grant agrément No. 8475–68), and Region Hauts-de-France for “CatBioInnov” project are also acknowledged. Mateus Freitas Paiva acknowledges the Program for Early stage in Lille (Pearl). Fabio B. Noronha thanks Fundação de Amparo à Pesquisa do Estado do Rio de Janeiro (FAPERJ-E-26/202.783/2017) and Conselho Nacional de Desenvolvimento Cientifico e Tecnológico (CNPq-303667/2018-4).

Data availability No datasets were generated or analysed during the current study.

Declarations

Conflict of interest The authors declare that they have no conflict of interest.

References

Acharya S, Liyanage S, Parajuli P, Parajuli P, Rumi SS, Abidi N (2021) Utilization of cellulose to its full potential: a review on cellulose dissolution, regeneration, and applications. Polymers 13:4344. https://doi.org/10.3390/polym13244344

Awosusi AA, Ayeni A, Adeleke R, Daramola MO (2017) Effect of water of crystallization on the dissolution efficiency of molten zinc chloride hydrate salts during the pre-treatment of corncob biomass. J Chem Technol Biotechnol 92:2468–2476. https://doi.org/10.1002/jctb.5266

Bodachivskyi I, Page CJ, Kuzhiumparambil U, Hinkley SFR, Sims IM, Williams BG (2020) Dissolution of cellulose: are ionic liquids innocent or noninnocent solvents? ACS Sustain Chem Eng 8:10142–10150. https://doi.org/10.1021/acssuschemeng.0c02204

Cao NJ, Xu Q, Chen CS, Gong CS, Chen LF (1994) Cellulose hydrolysis using zinc chloride as a solvent and catalyst. Appl Biochem Biotechnol 45–46:521–530. https://doi.org/10.1007/BF02941827

Chen Y, Yu H-Y, Li Y (2020) Highly efficient and superfast cellulose dissolution by green chloride salts and its dissolution mechanism. ACS Sustain Chem Eng 8:18446–18454. https://doi.org/10.1021/acssuschemeng.0c05788

Cheng M, Qin Z, Chen Y, Hu S, Ren Z, Zhu M (2017) Efficient extraction of cellulose nanocrystals through hydrochloric acid hydrolysis catalyzed by inorganic chlorides under hydrothermal conditions. ACS Sustain Chem Eng 5:4656–4664. https://doi.org/10.1021/acssuschemeng.6b03194

de Almeida RM, Li J, NederlofO’Çonnor CP, Makkee M, Moulijn JA (2010) Cellulose conversion to isosorbide in molten salt hydrate media. Chemsuschem 3:325–328. https://doi.org/10.1002/cssc.200900260

de Souza PM, de Sousa LA, Noronha FB, Wojcieszak R (2022) Dehydration of levoglucosan to levoglucosenone over solid acid catalysts. Tuning the product distribution by changing the acid properties of the catalysts. Molecular Catalysis 529:112564. https://doi.org/10.1016/j.mcat.2022.112564

Deng T, Cui X, Qi Y, Wnag Y, Hou X, Zhu Y (2012) Conversion of carbohydrates into 5-hydroxymethylfurfural catalyzed by $ZnCl_2$ in water. Chem Commun 48:5494. https://doi.org/10.1039/c2cc00122e

Deng W, Kennedy JR, Tsilomelekis G, Zheng W, Nikolakis V (2015) Cellulose hydrolysis in acidified LiBr molten salt hydrate media. Ind Eng Chem Res 54:5226–5236. https://doi.org/10.1021/acs.iecr.5b00757

Fischer S, Leipner H, Thümmler K, Brendler K, Peters J (2003) Inorganic molten salts as solvents for cellulose. Cellulose 10:227–236. https://doi.org/10.1023/A:1025128028462

Giannetto Pace G (2000) Zeolitas: características, propiedades y aplicaciones industriales. Editorial Innovacín Tecnológica, Facultad de Ingeniería, UCV, Caracas

Hou Q, Li W, Zhen M, Liu L, Chen Y, Yang Q, Huang F, Zhang S, Ju M (2017) An ionic liquid–organic solvent biphasic system for efficient production of 5-hydroxymethylfurfural from carbohydrates at high concentrations. RSC Adv 7:47288–47296. https://doi.org/10.1039/C7RA10237B

Hou Q, Qi X, Zhen M, Qian H, Nie Y, Bai C, Zhang S, Bai X, Ju M (2021) Biorefinery roadmap based on catalytic production and upgrading 5-hydroxymethylfurfural. Green Chem 23:119–231. https://doi.org/10.1039/D0GC02770G

Kim I, Kim J, Lee D (2014) A comparative study on catalytic properties of solid acid catalysts for glycerol acetylationat low temperatures. Appl Catal B Environ 148–149:295–303. https://doi.org/10.1016/j.apcatb.2013.11.008

Lara-Serrano M, Morales-delaRosa S, Campos-Martín JM, Fierro JLG (2020) High enhancement of the hydrolysis rate of cellulose after pretreatment with inorganic salt hydrates. Green Chem 22:3860–3866. https://doi.org/10.1039/D0GC01066A

Leipner H, Fischer S, Brendler E, Voigt W (2000) Structural changes of cellulose dissolved in molten salt hydrates. Macromol Chem Phys 201:2041–2049. https://doi.org/

10.1002/1521-3935(20001001)201:15%3c2041::AID-MACP2041%3e3.0.CO;2-E

Liang C, Du C, Wu X, Wang J, Xu J, Hu P, Qu W (2022) Comparison of corncob-derived solid acids and evaluation of catalytic cellulose hydrolysis performance in LiBr. Biomass Convers Biorefin. https://doi.org/10.1007/s13399-022-02322-6

Liu Q, Ma Q, Sabnis S, Zheng W, Vlachos DG, Fan W, Li W, Ma L (2019) Production of high-yield short-chain oligomers from cellulose: via selective hydrolysis in molten salt hydrates and separation. Green Chem 21:5030–5038. https://doi.org/10.1039/c9gc02297j

Liu Q, Luo S, Fan W, Ouyang X, Qiu X (2021a) Separation of short-chain glucan oligomers from molten salt hydrate and hydrolysis to glucose. Green Chem 23:4114–4124. https://doi.org/10.1039/D1GC00851J

Liu Q, Zhou L, Fan D, Guan M, Ma Q, Li S, Ouyang X, Qiu X, Fan W (2021b) Adsorption-enhanced glucan oligomer production from cellulose hydrolysis over hyper-cross-linked polymer in molten salt hydrate. ACS Appl Mater Interfaces 13:52082–52091. https://doi.org/10.1021/acsami.1c09360

Liu G, Xie Y, Wei C, Liu C, Song F, Sun X, Zhang Y, Cui H (2022) Synergistic catalysis of species in molten salt hydrate for conversion of cellulose to 5-hydroxymethylfurfural. Biomass Bioenergy 158:106363. https://doi.org/10.1016/j.biombioe.2022.106363

Ma Q, Guan M, Fan D, Jiang E (2022a) Production of high-yield 5-hydroxymethylfurfural from crystalline cellulose via one-pot conversion in molten salt hydrate/acetone and separation. Fuel 324:124678. https://doi.org/10.1016/j.fuel.2022.124678

Ma Q, Lin J, Guan M, Liang H, Liu Q (2022b) Enhanced cello-oligosaccharides production from cellulose hydrolysis in molten salt hydrate over lignin-based hyper-cross-linked polymer (LHCP) adsorption. Appl Catal A Gen 644:118808. https://doi.org/10.1016/j.apcata.2022.118808

Ni Y, Sun A, Wu X, Hai G, Hu J, Li T, Li G (2011) Preparation of hierarchical mesoporous Zn/HZSM-5 catalyst and its application in MTG reaction. J Nat Gas Chem 20:237–242. https://doi.org/10.1016/S1003-9953(10)60184-3

Nie Y, Hou Q, Bai C, Qian H, Bai X (2020) Transformation of carbohydrates to 5-hydroxymethylfurfural with high efficiency by tandem catalysis. J Clean Prod 274:123023. https://doi.org/10.1016/j.jclepro.2020.123023

Olsson C, Westm G (2013) Direct dissolution of cellulose: background, means and applications. In: van de Ven TGM, Godbout L (eds) Cellulose—fundamental aspects, IntechOpen, pp 143–178. https://doi.org/10.5772/52144

Paiva MF, Sadula S, Vlachos D, Wojcieszak R, Vanhove G, Noronha FB (2024) Advancing lignocellulosic biomass fractionation through molten salt hydrates: catalyst-enhanced pretreatment for sustainable biorefineries. Chemsuschem. e202400396 https://doi.org/10.1002/cssc.202400396

Rodriguez Quiroz N, Norton AM, Nguyen H, Vasileiadou E (2019a) Homogeneous metal salt solutions for biomass upgrading and other select organic reactions. ACS Catal 9:9923–9952. https://doi.org/10.1021/acscatal.9b01853

Rodriguez Quiroz N, Padmanathan AMD, Mushrif SH, Vlachos DG (2019b) Understanding acidity of molten salt hydrate media for cellulose hydrolysis by combining kinetic studies, electrolyte solution modeling, molecular dynamics simulations, and 13 C NMR experiments. ACS Catal 9:10551–10561. https://doi.org/10.1021/acscatal.9b03301

Sadula S, Oesterling O, Nardone A et al (2017) One-pot integrated processing of biopolymers to furfurals in molten salt hydrate: understanding synergy in acidity. Green Chem 19:3888–3898. https://doi.org/10.1039/c7gc01709j

Sang S, Chang F, Liu Z, He C, He Y, Xu L (2004) Difference of ZSM-5 zeolites synthesized with various templates. Catal Today 93–95:729–734. https://doi.org/10.1016/j.cattod.2004.06.091

Sen S, Martin JD, Argyropoulos DS (2013) Review of cellulose non-derivatizing solvent interactions with emphasis on activity in inorganic molten salt hydrates. ACS Sustain Chem Eng 1:858–870. https://doi.org/10.1021/sc400085a

Sen S, Losey BP, Gordon EE, Argyropoulos DS, Martin JD (2016) Ionic liquid character of zinc chloride hydrates define solvent characteristics that afford the solubility of cellulose. J Phys Chem B 120:1134–1141. https://doi.org/10.1021/acs.jpcb.5b11400

Sluiter A, Ruiz R, Scarlata C, Sluiter J, Templeton D (2008) Determination of Ash Content in Biomass - NREL/TP-510–42622

Sun L, Han J, Wu J, Huang W, Li Y, Mao Y, Wang L, Wang Y (2022) Cellulose pretreatment with inorganic salt hydrate: Dissolution, regeneration, structure and morphology. Ind Crops Prod 180:114722. https://doi.org/10.1016/j.indcrop.2022.114722

vom Stein T, Grande P, Sibilla F, Commandeur U, Fischer R, Leitner W, de Maria PD (2010) Salt-assisted organic-acid-catalyzed depolymerization of cellulose. Green Chem 12:1844–1849. https://doi.org/10.1039/c0gc00262c

Wang J, Cui H, Wang Y, Zhao R, Xie Y, Wang M, Yi W (2020) Efficient catalytic conversion of cellulose to levulinic acid in the biphasic system of molten salt hydrate and methyl isobutyl ketone. Green Chem 22:4240–4251. https://doi.org/10.1039/D0GC00897D

Wei W, Wu S (2017) Depolymerization of cellulose into high-value chemicals by using synergy of zinc chloride hydrate and sulfate ion promoted titania catalyst. Bioresour Technol 241:760–766. https://doi.org/10.1016/j.biortech.2017.06.004

Wu T, Li N, Pan X, Chen S-L (2020) Homogenous hydrolysis of cellulose to glucose in an inorganic ionic liquid catalyzed by zeolites. Cellulose 27:9201–9215. https://doi.org/10.1007/s10570-020-03411-3

Yang Y-J, Shin J-M, Kang TH, Kimura S, Wada M, Kim U-J (2014) Cellulose dissolution in aqueous lithium bromide solutions. Cellulose 21:1175–1181. https://doi.org/10.1007/s10570-014-0183-9

Yoo CG, Li N, Swannell M, Pan X (2017) Isomerization of glucose to fructose catalyzed by lithium bromide in water. Green Chem 19:4402–4411. https://doi.org/10.1039/C7GC02145C

Zeng M, Pan X (2022) Insights into solid acid catalysts for efficient cellulose hydrolysis to glucose: progress, challenges, and future opportunities. Catal Rev 64:445–490. https://doi.org/10.1080/01614940.2020.1819936

Zhang J, Nolte MW, Shanks BH (2014) Investigation of primary reactions and secondary effects from the pyrolysis of different celluloses. ACS Sustain Chem Eng 2:2820–2830. https://doi.org/10.1021/sc500592v

Zhang Y-R, Li N, Li M-F, Fan Y-M (2016) Highly efficient conversion of microcrystalline cellulose to 5-hydroxymethyl furfural in a homogeneous reaction system. RSC Adv 6:21347–21351. https://doi.org/10.1039/C5RA22129C

Zhang Y-R, Song Y-N, Chen C-Z, Li M-F, Zhang Z-T, Fan Y-M (2017) One-vessel synthesis of 5-hydroxymethylfurfural in concentrated zinc chloride solution from lignocellulosic materials. BioResources 12:7807–7818. https://doi.org/10.15376/biores.12.4.7807-7818

Zhou Z, Liu D, Zhao X (2021) Conversion of lignocellulose to biofuels and chemicals via sugar platform: an updated review on chemistry and mechanisms of acid hydrolysis of lignocellulose. Renew Sustain Energy Rev 146:111169. https://doi.org/10.1016/j.rser.2021.111169